Ecotoxicology and Environmental Safety 257 (2023) 114950

Contents lists available at ScienceDirect

Ecotoxicology and Environmental Safety

journal homepage: www.elsevier.com/locate/ecoenv

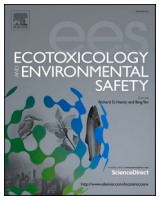

MiR-26a-5p from HucMSC-derived extracellular vesicles inhibits epithelial mesenchymal transition by targeting Adam17 in silica-induced lung fibrosis

Jing Zhao [a,b], Qiyue Jiang [a,b], Chunjie Xu [a,b], Qiyue Jia [a,b], Hongwei Wang [a,b], Wenming Xue [a,b], Yan Wang [a,b], Zhonghui Zhu [a,b], Lin Tian [a,b,*]

[a] Department of Occupational and Environmental Health, School of Public Health, Capital Medical University, Beijing 100069, China
[b] Beijing Key Laboratory of Environmental Toxicology, Capital Medical University, Beijing 100069, China

ARTICLE INFO

Keywords:
Silica
HucMSC-EVs
EMT
MiR-26a-5p
Adam17
Lung fibrosis

ABSTRACT

Silicosis is one of several potentially fatal occupational pathologies caused by the prolonged inhalation of respirable crystalline silica. Previous studies have shown that lung epithelial-mesenchymal transition (EMT) plays a significant role in the fibrosis effect of silicosis. Human umbilical cord mesenchymal stem cells-derived Extracellular vesicles (hucMSC-EVs) have attracted great interest as a potential therapy of EMT and fibrosis-related diseases. However, the potential effects of hucMSC-EVs in inhibiting EMT in silica-induced fibrosis, as well as its underlying mechanisms, remain largely unknown. In this study, we used the EMT model in MLE-12 cells and observed the effects and mechanism of hucMSC-EVs inhibition of EMT. The results revealed that hucMSC-EVs can indeed inhibit EMT. MiR-26a-5p was highly enriched in hucMSC-EVs but was down-regulated in silicosis mice. We found that miR-26a-5p in hucMSC-EVs was over-expressed after transfecting miR-26a-5p expressing lentivirus vectors into hucMSCs. Subsequently, we explored if miR-26a-5p, attained from hucMSC-EVs, was involved in inhibiting EMT in silica-induced lung fibrosis. Our findings suggested that hucMSC-EVs could deliver miR-26a-5p into MLE-12 cells and cause the inhibition of the Adam17/Notch signalling pathway to ameliorate EMT in silica-induced pulmonary fibrosis. These findings might represent a novel insight into treating silicosis fibrosis.

1. Introduction

Silicosis is classified as an occupational disease, which is caused by prolonged inhalation of respirable crystalline silica, which results in respiratory dysfunction and generalised lung fibrosis (Fan et al., 2022). Despite the long-term efforts by the WHO who have attempted to eliminate silicosis, the burden of silicosis remains high (The Lancet Respiratory, 2019). So far, although silicosis has a clear etiology, its complicated pathogenesis restricts its treatment options. As per published research findings, the underlying pathogenesis pertaining to silicosis pulmonary fibrosis constitutes of the impairment of alveolar epithelial cells, up-regulated activation of macrophage cells, increased fibroblast proliferation, and ultimately collagen deposition (Chanda et al., 2019). The progression of pulmonary fibrosis diseases is considered to be highly dependant on the degree of fibroblast proliferation (Wang et al., 2021). Previously, studies suggest that Epithelial Mesenchymal Transition (EMT) is considered as one source of fibroblasts (Duffield et al., 2013). During EMT, epithelial cells lose their epithelial proteins including E-cadherin and ZO1, subsequently, the cell converts into a mesenchymal phenotype as it gains mesenchymal markers such as Vimentin and α-smooth muscle actin (α-SMA) (Sheng et al., 2020). Multiple studies have put forward that Transforming growth factor-β1 (TGF-β1) is a general means to produce experimental silica-stimulated EMT and fibrosis (Cheng et al., 2021; Wang et al., 2017). We created the EMT model in silica-induced fibrosis by stimulating it with TGF-β1 in our previous study and the results showed that the inhibition of EMT down-regulated the expression of Col1a1 and α-SMA (Wang et al., 2021). Therefore, it seems that restraining the activation of EMT can affect the progress of pulmonary fibrosis.

Extracellular vesicles (EVs) including exosomes and microvesicles

Abbreviations: 3D, three-dimensional; Adam17, Disintegrin and metalloproteinase domain-containing protein 17; EMT, epithelial-mesenchymal transition; EVs, extracellular vesicles; H&E, hematoxylin and eosin; miRNA, micro RNA; TGF-β1, transforming growth factor-β1; ZO1, tight junction protein 1; α-SMA, alpha smooth muscle.

* Corresponding author at: Department of Occupational and Environmental Health, School of Public Health, Capital Medical University, Beijing 100069, China.
E-mail address: tian_lin@163.com (L. Tian).

https://doi.org/10.1016/j.ecoenv.2023.114950
Received 6 January 2023; Received in revised form 6 April 2023; Accepted 21 April 2023
Available online 24 April 2023

are involved in a spectrum of biological processes via delivering microRNAs (miRNAs), mRNAs, and proteins to target cells, are considered as important mediators of intercellular communication (Wiklander et al., 2015). Multiple studies have reported that the EVs form human umbilical cord mesenchymal stem cells (hucMSC-EVs) can carry biologically active molecules such as miRNAs that modulate the expression of EMT markers in recipient cells (Abbaszadeh et al., 2020; Li et al., 2021; Qiu et al., 2022; Yaghoubi et al., 2019). Meanwhile, our previous study found that hucMSC-EVs can ameliorate lung fibrosis and deliver let-7i-5p to inhibit fibroblast activation in silicosis (Xu et al., 2022). In a previous study, we identified miRNAs using high-throughput sequences between hucMSC-EVs and MRC-5-EVs (Xu et al., 2020). We revealed that the expression of miR-26a-5p was significantly enriched in hucMSC-EVs and down-regulated in silicosis mice. Recent research shows that miRNAs regulates EMT programs and ameliorates silicosis lung fibrosis by targeting key proteins (Qi et al., 2020). However, up to now, no study has investigated the mechanism of miR-26a-5p in the process of EMT during silicosis.

We identified that the interactions that occur between miR-26a-5p and Adam17 were involved in EMT (Chung et al., 2022; Shi et al., 2021; Sisto et al., 2021). As a member of the family of membrane-tethered disintegrins and metalloproteases, Adam17 is known to be a multifunctional proteinase (Calligaris et al., 2021). Studies show that Adam17 promotes idiopathic pulmonary fibrosis via EMT activation; they suggest that Adam17 plays a critical role in the regulation of the EMT and fibrosis (Sisto et al., 2021). Lu et al. identified that by inhibiting the expression of Adam17 the EMT process is reversed owing to the suppression of the Notch signalling pathway (Lu et al., 2019). The cleavage of Notch receptors, mediated by Adam17, is an important step in the activation of the Notch signalling pathway (Christian, 2012). Activation of Notch1 was shown to induce the transcriptional factor Snail expression, involved in TGF-β induced EMT (Saad et al., 2010). Here, our study aims to explore the function of hucMSC-EVs-delivered-miR-26a-5p in inhibiting EMT and ameliorating silicosis lung fibrosis. This process suggests that hucMSC-EVs might be used a beneficial therapeutic carrier used in silicosis.

2. Results

2.1. HucMSCs-EVs inhibits TGF-β1-induced EMT in MLE-12 cells

We expanded the growth of hucMSCs within eight days using the 3D dynamic culturing method (Fig. 1A). EVs from hucMSCs were isolated, characterised, and quantified by the same method we described in our previous study (Xu et al., 2020). The results demonstrated that hucMSCs are able to produce EVs. In our experiments we were able to isolate hucMSC-EVs.

To obtain insight into the effect of hucMSC-EVs, we initially determined whether hucMSC-EVs could be endocytosed into MLE-12 cells by PKH67 staining. The green fluorescent dye, PKH67-labeled hucMSC-EVs, were transferred into the MLE-12 cells (Fig. 1B). The results showed that MLE-12 cells exhibited the uptake of hucMSC-EVs. To determine whether hucMSC-EVs could inhibit EMT induced by TGF-β1 in MLE-12 cells. TGF-β1 was used to induce EMT in MLE-12 cells, which were then treated with hucMSC-EVs. QPCR and Western blotting results showed that compared with the control group, the downregulation of E-cadherin and ZO1 were accompanied with the upregulation of Vimentin and α-SMA in the TGF-β1 group; however, compared with the TGF-β1 group the levels of E-cadherin and ZO1 were increased and the levels of Vimentin and α-SMA were reduced in the TGF-β1 + hucMSC-EVs group (Fig. 1C-D). Immunofluorescence results showed that hucMSC-EVs treatment could increase the level of E-cadherin in MLE-12 cells (Fig. 1E). These data suggested that hucMSC-EVs could inhibit EMT induced by TGF-β1 in MLE-12 cells.

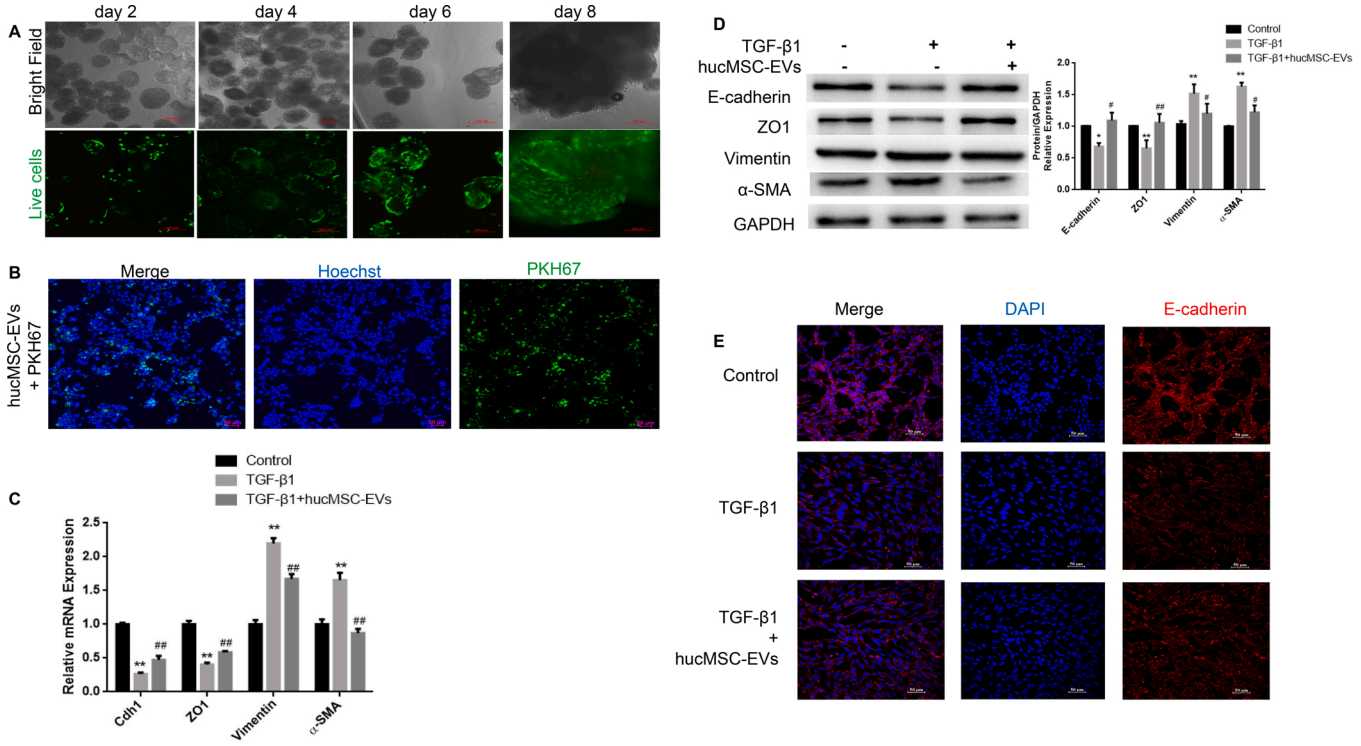

Fig. 1. hucMSC-EVs inhibited EMT induced by TGF-β1 in MLE-12 cells. (A) Representative image of hucMSCs on day 2, day 4, day 6 and day 8. Green: live cells. Scale bar: 200 μm. (B) Uptake of hucMSC-EVs by MLE-12 cells examined by laser scanning confocal microscope. Green: hucMSC-EVs. Blue: cell nucleus. Scale bar: 50 μm. (C-D) Detection of E-cadherin, ZO1, Vimentin and α-SMA expression in hucMSC-EVs by qPCR and Western blotting in MLE-12 cells. Cdh1: E-cadherin gene. (E) Immunofluorescence staining for E-cadherin in MLE-12 cells, Bule: cell nucleus, Red: E-cadherin, Scale bar: 50 μm. n = 3, * $p < 0.05$, * * $p < 0.01$ compared with the control group; # $p < 0.05$, ## $p < 0.01$ compared with the TGF-β1 group. All data are shown as means ± SD.

2.2. MiR-26a-5p derived from hucMSC-EVs was the key molecule related to EMT

To identify the miRNA expression and the mechanism for the therapeutic effects of hucMSC-EVs, miRNAs were screened by miRNAs high-throughput sequence (Xu et al., 2022). From our analyses, we identified 13 miRNAs involved in the intersection of significantly up-regulated miRNAs and high abundance miRNAs, from hucMSC-EVs (Abundance $>$ 5000 RPM, $\log_2$ (Fold_change) $>$ 1.5) (Fig. S1A, Table S1). By referring to published literature, we noticed that miR-148a-3p, miR-199a-3p, miR-26a-5p and miR-381–3p were related to EMT (Huang et al., 2020; Li et al., 2019; Liu et al., 2020; Wang et al., 2016). Meanwhile, we observed that the expression of miR-26a-5p was down-regulated in the lungs of silicosis mice and TGF-β1 stimulated MLE-12 cells (Fig. S1B-C). The treatment of hucMSC-EVs significantly increased the expression of miR-26a-5p (Fig. S1D). Thus, miR-26a-5p was possibly responsible for EMT and silicosis fibrosis, which was then selected as the key molecule.

2.3. HucMSC-EVs inhibited the TGF-β1-induced EMT by transferring miR-26a-5p to MLE-12 cells

To confirm if the role of miR-26a-5p, derived from hucMSC-EVs, contributes to inhibiting TGF-β1-induced EMT, we transfected hucMSCs with miR-26a-5p expression and repression lentivirus vectors to construct miR-26a-5p-overexpress and miR-26a-5p-inhibit transfected hucMSCs (Fig. 2A-B), respectively. The EVs isolated from miR-26a-5p-overexpressed transfected hucMSCs [EVs-miR-26a-5p(+)] exhibited high expression of miR-26a-5p, compared with the EVs isolated from negative control lentivirus vectors (NC) transfected hucMSCs (EVs-NC), and the EVs isolated from miR-26a-5p-inhibitor transfected hucMSCs [EVs-miR-26a-5p(-)] revealed a reduced expression of miR-26a-5p compared with EVs-NC (Fig. 2C-D). We analyzed the relative protein expression levels in the MLE-12 cells stimulated by TGF-β1, which were treated with hucMSC-EVs, EVs-NC or EVs-miR-26a-5p (+), respectively. In contrast to the TGF-β1 group, in the TGF-β1 + hucMSC-EVs group, protein levels of E-cadherin and ZO1 were seen to increase, while Vimentin and α-SMA decreased. E-cadherin and ZO1 levels were up-regulated, compared with the TGF-β1 + EVs-NC group; moreover, the levels of Vimentin and α-SMA were down-regulated in the TGF-β1 + EVs-miR-26a-5p(+) group (Fig. 2E). Therefore, our results show that the up-regulation of miR-26a-5p enhances the hucMSC-EVs effects of preventing the TGF-β1-induced EMT. However, when EVs-NC or EVs-miR-26a-5p(-) were administered to MLE-12 cells stimulated with TGF-β1, EVs-miR-26a-5p(-) markedly attenuated the increase of E-cadherin and ZO1 whilst limiting the decrease of Vimentin and α-SMA in the EVs-NC treatment group (Fig. 2F). The results showed that downregulation of miR-26a-5p could blunt the hucMSC-EVs effects of inhibiting TGF-β1-induced EMT. These results indicated that hucMSC-EVs suppressed TGF-β1-induced EMT by delivering miR-26a-5p to MLE-12 cells.

2.4. MiR-26a-5p inhibited TGF-β1-induced EMT in MLE-12 cells through Adam17/Notch signalling pathway

In order to further explore the underlying mechanism by which TGF-β1-induced EMT is regulated by miR-26a-5p, we used online databases

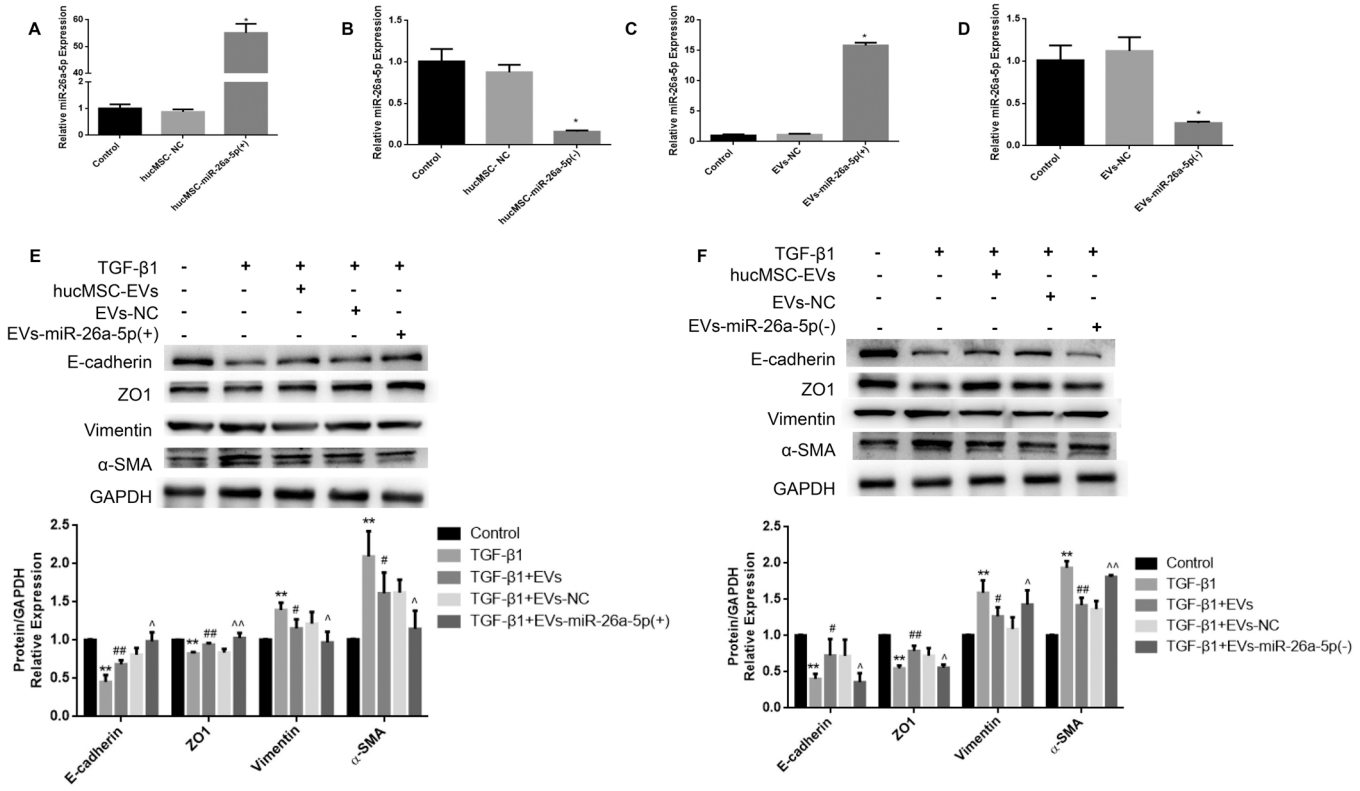

Fig. 2. HucMSC-EVs suppressed the TGF-β1-induced EMT progression by transferring miR-26a-5p to MLE-12 cells in vitro. (A-B) The levels of miR-26a-5p in hucMSC cells transfected with expressing and repressing lentivirus vectors were determined by qPCR. n = 3, * $p < 0.05$ compared with the hucMSC-NC group. hucMSC-miR-26a-5p(+): miR-26a-5p-overexpress transfected hucMSCs; hucMSC-miR-26a-5p(-): miR-26a-5p-inhibit transfected hucMSCs. (C-D) The levels of miR-26a-5p in EVs derived from hucMSC cells transfected with expressing and repressing lentivirus vectors were determined by qPCR. n = 3, * $p < 0.05$ compared with the EVs-NC group. (E) Western blotting analysis of E-cadherin, ZO1, Vimentin and α-SMA in MLE-12 cells treated with hucMSC-EVs, EVs-NC or EVs-miR-26a-5p(+). (F) Western blotting analysis of E-cadherin, ZO1, Vimentin and α-SMA in MLE-12 cells treated with hucMSC-EVs, EVs-NC or EVs-miR-26a-5p(-). n = 3, * $p < 0.05$, * * $p < 0.01$ compared with the control group; # $p < 0.05$, ## $p < 0.01$ compared with the TGF-β1 group; ^ $p < 0.05$, ^^ $p < 0.01$ compared with the TGF-β1 + EV-NC group. All data are shown as means ± SD.

to predict the potential target of miR-26a-5p that may participate in the regulation of EMT. Overlap analysis suggested that Adam17 was the potential target of miR-26a-5p. The 3′ UTR seed region sequence (UACUUGA) of Adam17 was complementary to miR-26a-5p (Fig. S2A). Next, we conducted luciferase reporter assays by using plasmids that contain wild-type or mutant Adam17 3′ UTRs with miR-26a-5p binding sites. Notably, dual luciferase reporter assays demonstrated reduced luciferase activity in the WT-miR-26a-5p group (Fig. 3A). Furthermore, the activity of Adam17-MUT luciferase reporter was not affected by the miR-26a-5p overexpressed vector. Therefore, we speculated that Adam17 was a potential target of miR-26a-5p in TGF-β1-induced EMT. To explore the exact effects of miR-26a-5p, we detected the protein expression levels of Adam17, Notch1, Hes1 and Snail in MLE-12 cells. The results showed that compared with the control group, the protein expressions of Adam17, Notch1, Hes1 and Snail were up-regulated in the TGF-β1 group; hucMSC-EVs treatment significantly inhibited their expressions. In contrast to the TGF-β1 + EVs-NC group, these levels were down-regulated in the EVs-miR-26a-5p(+) group (Fig. 3B), whereas EVs-miR-26a-5p(-) produced an opposite results (Fig. S2B).

Additionally, we used recombinant lentivirus to knockdown or overexpress Adam17 in MLE-12 cells (Fig. 3C, S2C). The results revealed that knockdown of the expression of Adam17 could down-regulate the expressions of Notch1, Hes1 and Snail, meanwhile promoting the expressions of E-cadherin and ZO1, as well as inhibiting the expressions of Vimentin and α-SMA (Fig. 3D-E). Subsequently, to further observe the function of Adam17 in TGF-β1-induced EMT, we transfected MLE-12 cells with miR-26a-5p mimics and over expressed Adam17 lentivirus. Compared with the TGF-β1 + Adam17-NC+miR-26a-5p mimics group, the levels of E-cadherin and ZO1 decreased, but the levels of Vimentin, α-SMA, Adam17, Notch1, Hes1 and Snail increased in the TGF-β1 + Adam17-OE+miR-26a-5p mimics group (Fig. S2D). Our results showed that overexpressed Adam17 reduces the miR-26a-5p mimics effects of preventing the TGF-β1-induced EMT, as well as blocking the Adam17/Notch signalling pathway. The aforementioned results suggest that miR-26a-5p derived from hucMSC-EVs inhibit TGF-β1-induced EMT by targeting Adam17 and blocking the Notch signalling pathway.

2.5. Silica-induced damage to respiratory function in silicosis Mice alleviated by EVs-miR-26a-5p(+)

To evaluate the metabolic processes of EVs-miR-26a-5p(+) in a silica-induced pulmonary fibrosis mice model, we monitored the migration of DiR-labeled EVs-miR-26a-5p(+) in mice. Bioluminescence imaging showed that the fluorescence in the lung was observed at 24 h and intensity increased gradually, reaching a maximum value at 72 h, then intensity gradually weakened, and disappeared at 120 h (Figs. 4A and S3A). Therefore, our results point out that EVs-miR-26a-5p(+) can indeed reach the lung tissue. The time interval of EVs-miR-26a-5p(+) injected was every 96 h, which ensures the continuous presence of EVs-miR-26a-5p(+) in vivo.

To investigate whether miR-26a-5p contributed to the hucMSC-EVs mediated therapeutic effect of silicosis fibrosis, we injected EVs-miR-26a-5p(+) into silica-induced pulmonary fibrosis mice model (Fig. 4B). To investigate the progression of respiratory diseases, we investigated the effect of silica and EVs-miR-26a-5p(+) on lung function. The five models: the standard model of TLC (total lung capacity), Snap Shot, Prime wave, FEV0.1 (the forced expiratory volume in 0.1 s) and the PV (pressure-volume) loops model, were all utilised to measure the mice lung functions. For the TLC model, Inspiratory capacity (IC), was reduced in the silica group, but raised in the EVs-miR-26a-5p(+) treatment group (Fig. 4C). For the Snap Shot model, silica increased respiratory resistance (Rrs) and elastic resistance (Ers), whilst it significantly

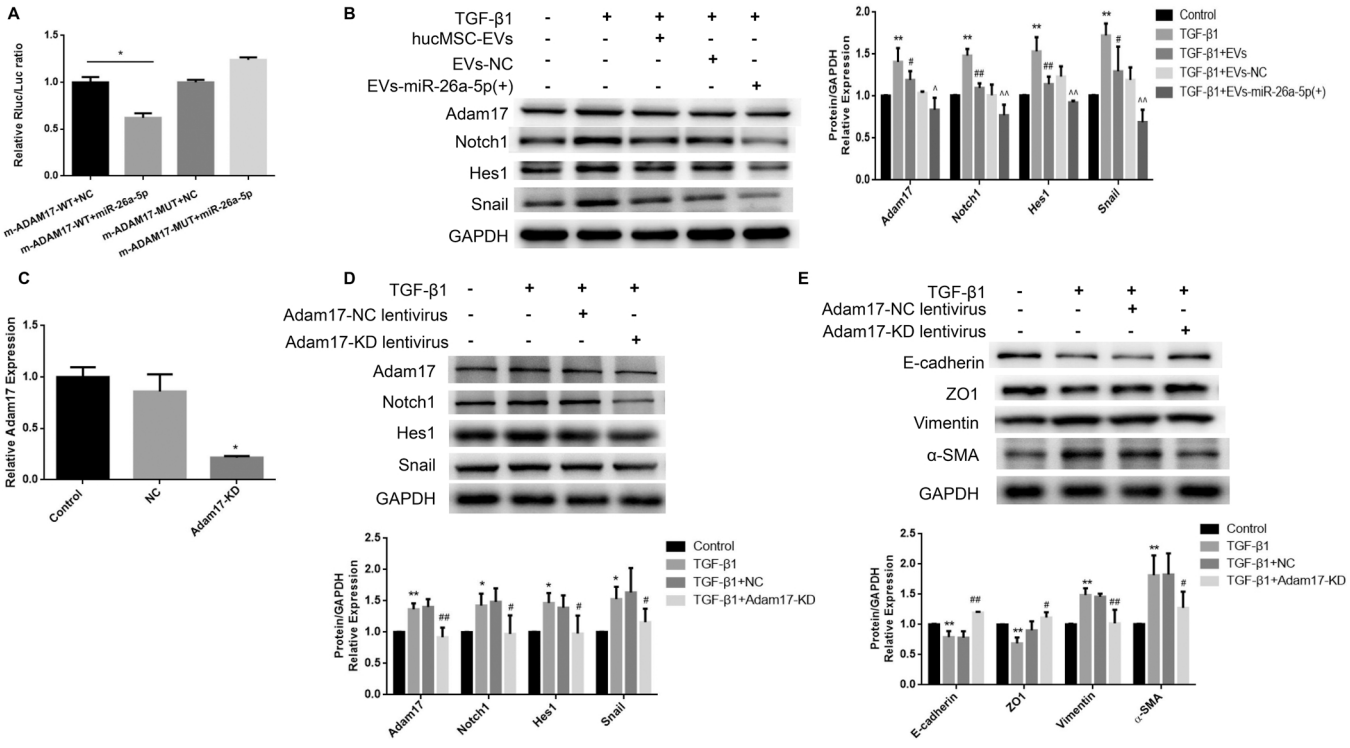

Fig. 3. MiR-26a-5p inhibited TGF-β1-induced EMT in MLE-12 cells through Adam17/Notch signaling pathway. (A) Luciferase activity of Adam17–3′UTR-WT and Adam17–3′UTR-MUT in cells in the presence of miR-26a-5p detected by dual-luciferase reporter gene assay. n = 3, * $p < 0.05$ compared with the WT-NC group. (B) Western blotting analysis the expression levels of Adam17, Notch1, Hes1 and Snail in MLE-12 cells treated with EVs-miR-26a-5p(+). n = 3, * $p < 0.05$, * * $p < 0.01$ compared with the control group; # $p < 0.05$, ## $p < 0.01$ compared with the TGF-β1 group. ^ $p < 0.05$, ^^ $p < 0.01$ compared with the TGF-β1 + EVs-NC group. (C) Knockdown recombinant lentivirus were transfected into MLE-12 cells. n = 3, * $p < 0.05$ compared with the NC group. KD: knockdown. (D-E) Western blotting analysis the expression levels of Adam17, Notch1, Hes1, Snail, E-cadherin, ZO1, Vimentin and α-SMA in MLE-12 cells. n = 3, * $p < 0.05$, * * $p < 0.01$ compared with the control group; # $p < 0.05$, ## $p < 0.01$ compared with the TGF-β1 + NC group.

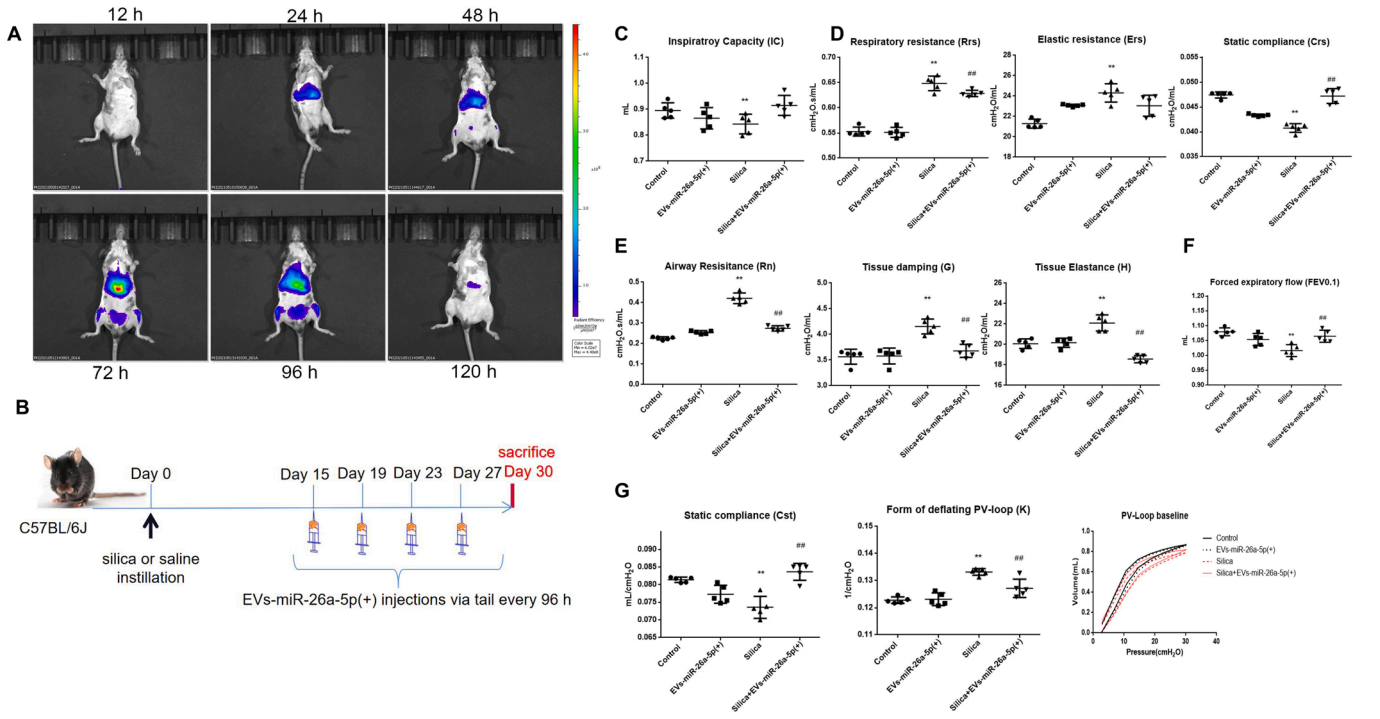

Fig. 4. EVs-miR-26a-5p(+) improved the respiratory function damaged by silica in mice. (A)The fluorescent signals were captured at different time points after injected with DiR-labeled EVs-miR-26a-5p(+) in images. (B) A schematic diagram illustrating the experimental design. (C) TLC model including inspiratory capacity. (D) The Snap Shot model including respiratory resistance, elastic resistance and static compliance. (E) The Prime wave model including airway resistance, tissue damping and tissue elastance. (F) The FEV0.1 model including forced expiratory flow in the first 0.1 s (G) The PV loops model including static compliance, form of deflating PV-loop and PV-loop baseline. n = 6, ** $p < 0.01$ compared with the control group; ## $p < 0.01$ compared with the silica group. All data are shown as means ± SD.

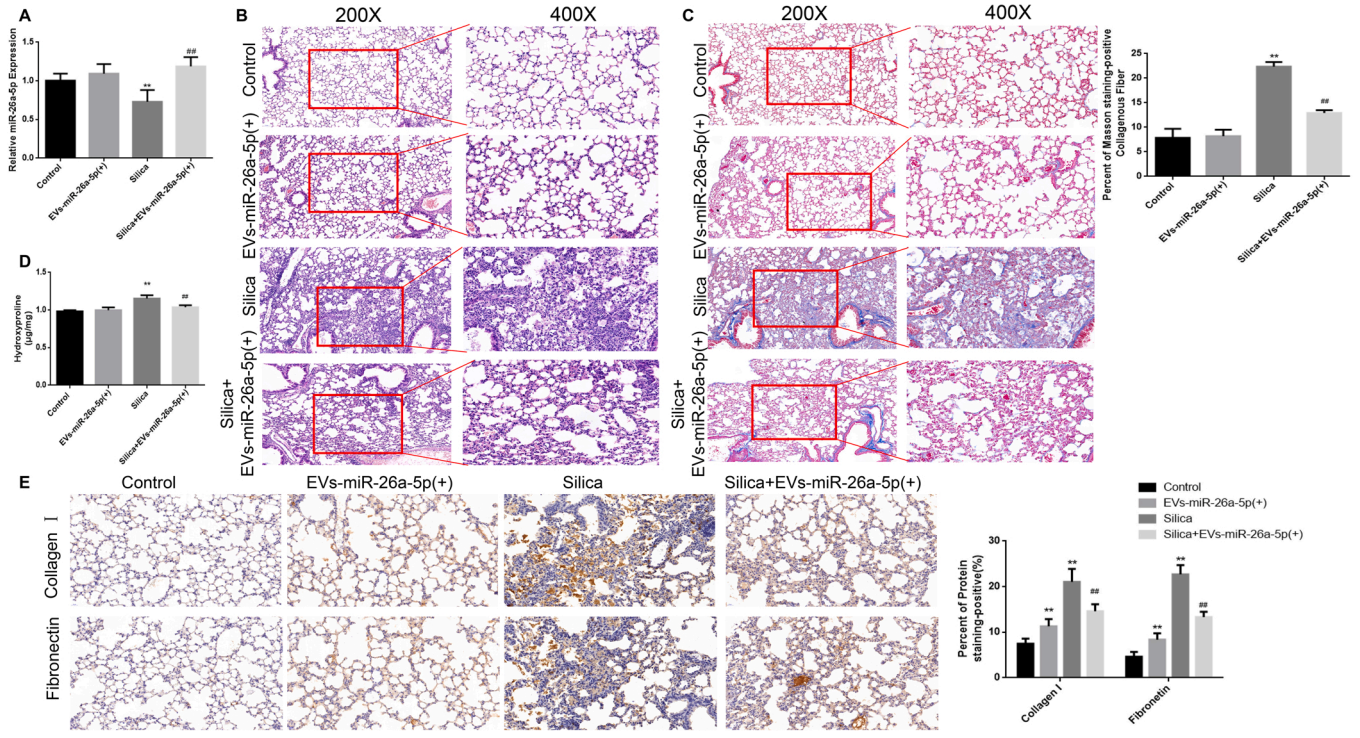

Fig. 5. EVs-miR-26a-5p(+) ameliorated silica-induced pulmonary fibrosis in mice. (A) The level of miR-26a-5p in lungs of mice determined by quantitative PCR. (B-C) H&E and Masson staining in the lungs of the mice in each group at 30 days (light micrograph magnifications of 200 × and 400 ×). (D) The content of HYP was increased in the silica group but decreased in the silica+EVs-miR-26a-5p(+). (E) Immunohistochemical staining was performed, and the levels of Collagen I and Fibronectin were determined in mice, light micrograph magnifications of 400 × , Scale bar: 20 μm. n = 6, * $p < 0.05$, ** $p < 0.01$ compared with the control group; # $p < 0.05$, ## $p < 0.01$ compared with the silica group. All data are shown as means ± SD.

reduced the respiratory system static compliance (Crs); but EVs-miR-26a-5p(+) treatment weakened the above changes induced by silica (Fig. 4D). For the Prime wave model, compared with the control group, Central airway resistance (Rn), tissue damping (G) and tissue elastance (H) were increased in the silica group. In contrast, in the silica+EVs-miR-26a-5p(+) group these effects declined (Fig. 4E). Silica reduced the FEV0.1, and EVs-miR-26a-5p(+) treatment increased this value (Fig. 4F). For the PV loops model, static compliance (Cst) was decreased by silica, mean whilst the form of deflating PV-loop (K) was increased. Notably, EVs-miR-26a-5p(+) treatment restored these changes. Moreover, we observed a downward trend of the PV-loop baseline of mice in the silica group, which is indicative of existing lung fibrosis. The silica+EVs-miR-26a-5p(+) mice displayed an upward shift, compared to the silica mice (Fig. 4G). Taken together, these results confirmed that EVs-miR-26a-5p(+) could attenuate silica-induced respiratory function damage in silicosis mice.

2.6. EVs-miR-26a-5p(+) ameliorated lung fibrosis in mice after silica exposure

To confirm whether EVs-miR-26a-5p(+) had a therapeutic effect of silicosis fibrosis in mice. The mice were sacrificed on the 30th day after silica instillation. By using qPCR analysis, we investigated that silica decreased the expression of miR-26a-5p, while EVs-miR-26a-5p(+) upregulated the expression of miR-26a-5p in the lungs of mice (Fig. 5A). The H&E and Masson staining results revealed that the silica group, in contrast to the control group, had a marked increase in the extent of interstitial lung fibrosis, the number of cell nodules, as well as the degree of collagen deposition. Mean-whilst, in the EVs-miR-26a-5p(+) group, we observed a reduction in the number of cell nodules and the total area of the blue fibers (Fig. 5B-C). Following silica treatment, the hydroxyproline concents in the lung was increased, however, EVs-miR-26a-5p(+) treatment blunted this effect (Fig. 5D). In addition, silica exposure significantly up-regulated the expressions of Collagen I and Fibronectin, meanwhile, after treatment with EVs-miR-26a-5p(+), the expressions of Collagen I and Fibronectin were significantly reduced (Fig. 5E). The results showed that EVs-miR-26a-5p(+) have potential effects to alleviate lung fibrosis in mice after silica exposure.

2.7. EVs-miR-26a-5p(+) blocks the Adam17/Notch signalling pathway to ameliorate EMT in silica-induced pulmonary fibrosis

After confirming the therapeutic effect of EVs-miR-26a-5p(+) in silica-induced pulmonary fibrosis in vivo, we further explored its underlying mechanism of action. We observed that on day 30, Silica induces a clear EMT, and EVs-miR-26a-5p(+) treatment ameliorated silica-induced EMT by restoring E-cadherin and by inhibiting the expression of α-SMA (Fig. 6A). Immunofluorescence observed that the expression of E-cadherin decreased and Vimentin increased in the lungs of the mice after silica instillation, whereas EVs-miR-26a-5p(+) treatment ameliorated these changes (Fig. 6B). The result of immunohistochemical staining showed that the level of Adam17 was increased in the silica group, which was decreased after EVs-miR-26a-5p(+) treatment (Fig. 6C). We further studied the effects of EVs-miR-26a-5p(+) on the Adam17/Notch signalling pathway. Western blotting results demonstrated that the expressions of Adam17, Notch1 and Hes1 were significantly higher owing to silica instillation, whereas EVs-miR-26a-5p(+) treatment inhibited these changes (Fig. 6D). These findings suggest that EVs-miR-26a-5p(+) ameliorate EMT in silica-induced pulmonary fibrosis by blocking the Adam17/Notch signalling pathway.

3. Discussion

Despite much research has been conducted in the underlying

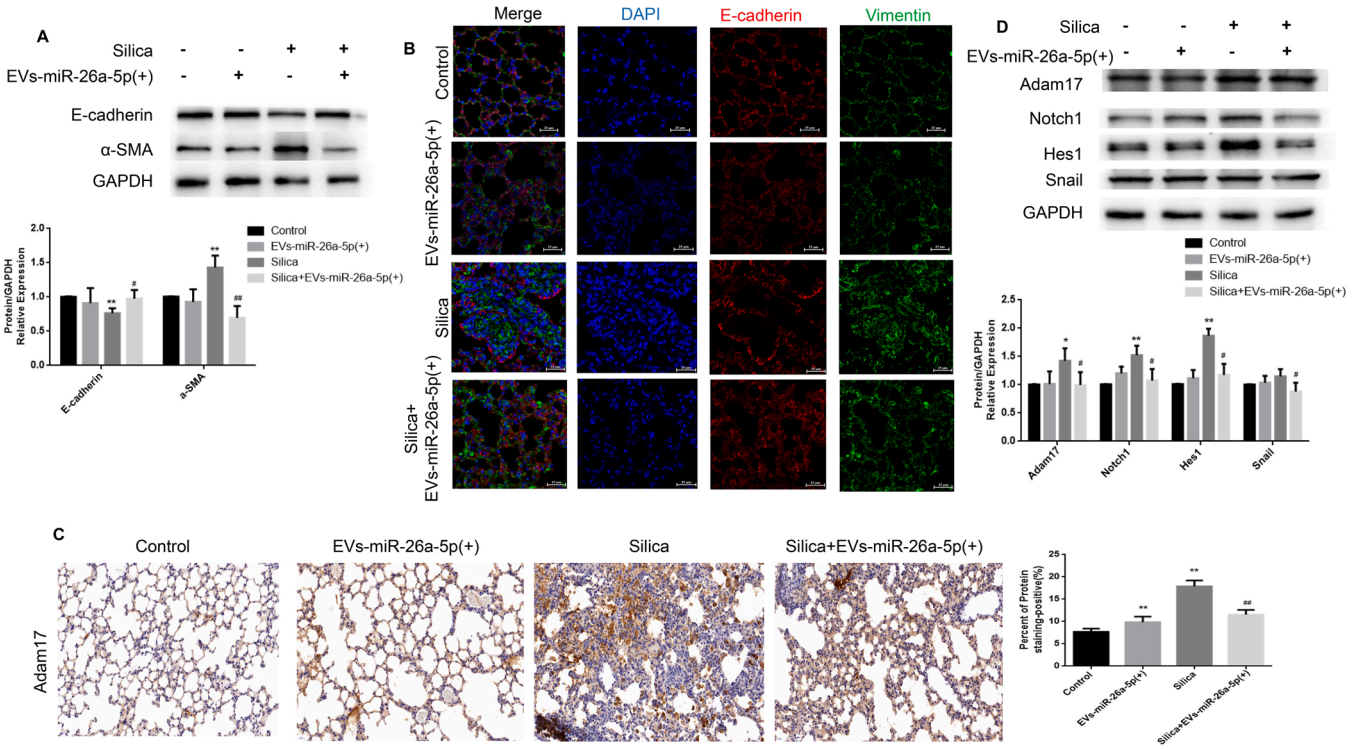

Fig. 6. EVs-miR-26a-5p(+) inhibited EMT in silica-induced pulmonary fibrosis mice. (A) Western blotting analysis the expression levels of E-cadherin and α-SMA in lung tissue. (B) Immunofluorescence staining in lung tissue, Scale bar: 25 μm. Bule: cell nucleus, Red: E-cadherin, Green: Vimentin. (C) Immunohistochemical staining was performed, and the level of Adam17 was determined in mice (light micrograph magnifications of 400 ×), Scale bar: 20 μm. (D) Western blotting analysis the expression levels of Adam17, Notch1, Hes1 and Snail in lung tissue. n = 6, $*p < 0.05$, $**p < 0.01$ compared with the control group; # $p < 0.05$, ## $p < 0.01$ compared with the silica group. All data are shown as means ± SD.

mechanism of silicosis, producing effective treatment to tackle silica-induced fibrotic diseases remains challenging. In the present study, we investigated that miR-26a-5p from hucMSC-EVs was associated with inhibiting EMT in silica-induced lung fibrosis.

Silicosis results from the inhalation of crystalline silica dust, consequently resulting in lung tissue inflammation and ultimately leading to fibrosis. Recently, mesenchymal stem cells (MSC) transplantation has received attention after demonstrating its potential use to treat silicosis (Chen et al., 2018). We have pointed out, in previous studies, that bone marrow mesenchymal stem cells (BMSC) attenuate silicosis fibrosis and protect damaged epithelial cells, and also suggested that the possible therapeutic mechanisms of BMSC relate to paracrine effects (Li et al., 2017). However, recent research shows that after tail vein intravenous of MSC transfusion in mice, only a small subset of MSC may redistribute to sites of injury and the bulk of MSC were trapped in the lung microvasculature (Sensebé and Fleury-Cappellesso, 2013). And another study describes the generation of antibodies against and immune rejection of allogeneic donor MSC and suggests that allo-rejection and transplantation shock would be the potential risks in MSC therapy (Ankrum et al., 2014). To minimise patient risk and overcome the disadvantage of MSC, MSC secreted extracellular vesicles (MSC-EVs), interacting with target cells and delivering their contents, are important for MSC to impart their ultimate therapeutic effect through the paracrine mechanism (Wiklander et al., 2019).

Extracellular vesicles (EVs) are cell secreted membrane structures, which have a diameter of 40–150 nm (Cocozza et al., 2020). In our study, the size of EVs, derived from hucMSC-EVs particles, displayed an average diameter of 128.2 nm as assessed with NTA; it suggests that EVs extracted from the cell supernatant mostly comprised of exosomes. Recent studies indicate that MSC-EVs could be an alternative agent to MSC therapy in regenerative medicine (Wiklander et al., 2019). Some preclinical studies have confirmed that MSC-EVs act as a novel therapy to treat fibrotic diseases (Huang and Yang, 2021; Zhang et al., 2020). Overall, cell-free therapy using MSC-EVs is an active and emerging field in regenerative medicine.

Our previous findings sustained that EMT was linked to the initiation and progression of silicosis fibrosis (Wang et al., 2021). Among the extracellular cytokines that activated EMT, TGF-β1, which was the primary factor driving fibrosis, could induce alveolar epithelial cells to undergo EMT in vivo and in vitro (Kasai et al., 2005; Kim et al., 2006). In this study, we stimulated MLE-12 cells with TGF-β1, which resulted in the decreased expression of E-cadherin and ZO1, and increased expression of Vimentin and α-SMA. After the cells were treated with hucMSC-EVs, the data suggested that hucMSC-EVs inhibit EMT induced by TGF-β1 in MLE-12 cells.

A recent study has reported that MSC-EVs could carry biologically active molecules including miRNAs that modulate the expression of EMT markers by targeting the key proteins in recipient cells (Li et al., 2022). Similarly, we noted that miR-26a-5p was markedly up-regulated and had a high abundance in hucMSC-EVs by a high-throughput sequence. Mean whilst miR-26a-5p was down-regulated in silicosis mice and in TGF-β1-induced EMT in MLE-12 cells. It is however worth mentioning that the level of miR-26a-5p increased after treatment with hucMSC-EVs. Thus, MiR-26a-5p derived from hucMSC-EVs was selected as the key molecule. MiR-26a is a member of the miR-26 family (Zhang et al., 2012). Previous research reported that miR-26a-5p played an important role in the regulating fibrosis-related diseases (Liang et al., 2016). In further studies miR-26a-5p was proven to have a strong association with EMT. Ma et al. discovered that Vimentin expression is up-regulated and E-cadherin are down-regulated when there is low expression of miR-26a (Ma et al., 2016). In a study conducted by Liang et al. forced expression of miR-26a was seen to alleviate TGF-β1-induced EMT (Liang et al., 2014). However, the role of miR-26a-5p from hucMSC-EVs in silica induced EMT and lung fibrosis remains largely unknown. In the present study, we used miR-26a-5p expression and repression lentivirus vectors to transfected hucMSCs respectively, then isolated the EVs-miR-26a-5p(+) and EVs-miR-26a-5p(-). EVs--miR-26a-5p(+) enhanced the effect of inhibiting EMT, however, EVs-miR-26a-5p(-) reversed the treatment effect by EVs-NC in MLE-12 cells. In a word, our study showed that after transfection and increased expression of miR-26a-5p, EVs-miR-26a-5p(+) were able to suppress TGF-β1-induced EMT by delivering miR-26a-5p to MLE-12 cells.

Adam17 plays an important role in various biological processes including cell signalling, adhesion and cellular migration (Calligaris et al., 2021). Ge et al. clarified that Adam17 was highly expressed in IPF patients and interstitial lung diseases patients (Ge et al., 2020). Further researches have shown that Adam17 could promote pulmonary fibrosis via EMT activation and inhibiting the expression of Adam17 could reverse EMT (Sisto et al., 2021). Lu et al. found that inhibiting the expression of Adam17 could reverse the EMT process through suppressing the Notch signalling pathway (Lu et al., 2019). In this study, we used recombinant lentivirus to knockdown or over-express Adam17 in MLE-12 cells. The results showed that knockdown of the expression of Adam17 could inhibit TGF-β1-induced EMT and suppress the activation of the Notch signalling pathway. Meanwhile, over-expression of Adam17 could reduce the miR-26a-5p mimics effects of preventing the TGF-β1-induced EMT and blocking the Notch signalling pathway. In the present study, we demonstrated that miR-26a-5p from hucMSC-EVs could inhibit TGF-β1-induced EMT by targeting Adam17. In the next step, we will use a human lung epithelial cell line to assess the signalling pathway in silicosis. This is also the limitation of this manuscript.

Consistent with these findings, in silicosis mice models, we observed that EMT and pulmonary fibrosis could be reduced after multiple tail intravenous injections of EVs-miR-26a-5p(+). To establish the experimental silicosis model, C57BL/6 J mice were exposed with intratracheal instillation of silica suspension, consistent with previous research (Sun et al., 2019; Xu et al., 2020). Recent studies showed that both intratracheal and intravenous routes could transfer EVs to treat pulmonary diseases but the intravenous route was the most widely used strategy in vivo (Yang et al., 2022). Because of its simplicity and repeatability, the intravenous route was the preferred method of administration of EVs for our study. Based on the assessment of bioluminescence imaging signals showed that the fluorescence intensity had been reduced on the 96 h after injection, and the signal disappeared on the 120 h. Therefore, we injected EVs-miR-26a-5p(+) every 96 h to ensure the presence of EVs-miR-26a-5p(+) in vivo.

We further evaluated the effect of silica and EVs-miR-26a-5p(+) on lung function in mice. For the purpose of clinical diagnosis and use in mouse models of lung fibrosis diseases, lung function tests have already been adopted (Nikitopoulou et al., 2019). In the present study, silica exposure increased Rrs, Ers and Rn, but decreased IC, Crs, FEV0.1 and Cst in mice. However, total lung capacity was almost unchanged in mice. Consistent with a previous study, Cao et al. tested lung function of mice, the results showed that Rrs and Ers increased, but IC decreased in mice after silica intratracheal instillation (Cao et al., 2022). At the same time, EVs-miR-26a-5p(+) could alleviate Rrs and Rn, indicating the possible therapeutic effect that EVs-miR-26a-5p(+) could have on both tissues and airways. EVs-miR-26a-5p(+) up-regulate IC, Crs, FEV0.1 and Cst, which indicate that EVs-miR-26a-5p(+) help to re-establish the compliance and elasticity of the lung parenchyma. EVs-miR-26a-5p(+) create an upward shift to the baseline of the PV loop, which suggests an upswing of the elastic recoil. These results showed that EVs-miR-26a-5p (+) could attenuate silica induced damage to respiratory function in mice.

Additionally, the present study indicated that EVs-miR-26a-5p(+) decreased lung fibrosis significantly. EVs-miR-26a-5p(+) treatment blocked EMT in silica-induced fibrosis by restoring E-cadherin and inhibiting Vimentin, α-SMA, Collagen I and Fibronectin. We discovered that silica significantly increased the expression of Adam17, Notch1 and Hes1 in mice, and that EVs-miR-26a-5p(+) treatment inhibited these changes. In a word, our study suggested that EVs-miR-26a-5p(+) might

ameliorated EMT in silica-induced lung fibrosis by blocking the Adam17/Notch signalling pathway.

In conclusion, our study discovered that up-regulation of miR-26a-5p in hucMSC-EVs could deliver miR-26a-5p into MLE-12 cells and result in blocking the Adam17/Notch signalling pathway to ameliorate EMT in silica-induced pulmonary fibrosis. Ultimately, these findings have a potential value for the development of a new therapeutic strategy in silica-induced pulmonary fibrosis.

4. Material and methods

4.1. Cell culture and treatment

Mouse type II alveolar epithelial cells (MLE-12) were maintained in DMEM containing 10% fetal bovine serum (Gibco, USA) under 5% CO_2 at 37 ℃. MLE-12 cells were stimulated by 5 ng/mL recombinant human TGF-β1 (Peprotech, NJ, USA) for 24 h, then treated with 50 μg/mL hucMSC-EVs for 24 h.

Additional details of hucMSCs culture have been previously described (Xu et al., 2020).

4.2. Isolation and analysis of EVs

The culture medium was collected and centrifuged at 2000g and 4 ℃ for 10 min, followed by centrifugation at 10000g and 4 ℃ for 30 min again. At which point we collected the supernatant and filtered it through a 0.22 μm filter membrane (Millipore, Billerica, USA). The resulting supernatants were concentrated using a 100 kDa centrifugal filter devices (Millipore, Billerica, USA) at 4000g for 20 min and centrifuged at 100000g and 4 ℃ for 70 min

The isolated EVs were observed by transmission electron microscope (TEM, Hitachi, Japan) and assessed with Western blotting. Additionally, the size of EVs were measured by nanoparticle tracking analysis (NTA, ZetaVIEW, PARTICLE METRIX).

4.3. In vitro tracking

HucMSC-EVs were labeled with PKH67 lipophilic membrane green fluorescent dye (Umibio, Shanghai, China) by the manufacturer's instructions. Details of the methods are provided in the supplementary material.

4.4. Antibodies and reagents

Antibodies used were CD81 (ab33697, Abcam, USA), TSG101 (ab125011, Abcam, USA), CD63 (25682–1-AP, proteintech, USA), Calnexin (ab92573, Abcam, USA), E-cadherin (ab76055, Abcam, USA), ZO1 (21773–1-AP, proteintech, USA), Vimentin (ab92547, Abcam, USA), α-SMA (ab7817, Abcam, USA), Adam17 (YC0076, immunoway, USA), Notch1 (ab52627, Abcam, USA), Hes1 (11988, Cell Signaling Technology, USA), Snail (AP2054a, Abcepta, USA), and GAPDH (2118, Cell Signaling Technology, USA).

4.5. Quantitative PCR (qPCR)

The total RNA from hucMSC-EVs, cultured cells and lung tissue of mice was isolated by Trizol reagent (Thermo Fisher Scientific, USA) under the manufacturer's instruction. Details of the methods are provided in the supplementary material.

4.6. MiRNA Transfection

After been stimulated by TGF-β1 for 24 h, MLE-12 cells were transfected with 50 nM of either miR-26a-5p mimics or NC mimics (Sangong Biotech, China) using Lipofectamine RNAiMAX Reagent (Invtrogen, USA) according to the manufacturer's instruction. The miR-26a-5p mimics sense was 5′-UUCAAGUAAUCCAGGAUAGGCU-3′ and the antisense was 5′-CCUAUCCUGGAUUACUUGAAUU-3′.

4.7. Establishment of cell lines

Lentivirus vectors expressing miR-26a-5p, repressing miR-26a-5p, knockdown and overexpression lentiviruses for Adam17, were all purchased from Genechem Corporation (Shanghai, China). Transfection in MLE-12 cells was performed according to the manufacturer's instructions.

4.8. Animal model and experimental design

60 male C57BL/6 J mice, which were purchased from Vital River Laboratory Animal Technology (Beijing, China,weight rang 20–22 g), were randomly subdivided into four groups: control group; EVs-miR-26a-5p(+) group; silica group; and silica+EVs-miR-26a-5p(+) group. Details of the methods are provided in supplementary material. The mice were euthanised on day 30 (protocol summarised in Fig. 4B). The Capital Medical University of Laboratory Animal Care and Use Committee approved this study (AEEI-2018–223). All efforts were made to minimise the suffering of the animals.

4.9. In vivo tracking

Mice were injected with EVs-miR-26a-5p(+) labeled with fluorescent DiR. We used the IVIS Spectrum imaging system (PerkinElmer, USA) to capture the fluorescent signal at 12 h, 24 h, 48 h, 72 h, 96 h, and 120 h in mice. Details of all methods are provided in the supplementary material.

4.10. Lung function measurements

Respiratory function measurements of mice were collected using the flexiVent FX system (SCIREQ, Montreal, Canada). Additional details of lung function measurement have been previously described (Xu et al., 2020).

4.11. Statistical analysis

All statistical analyses were performed using the SPSS software, version 20.0 (SPSS, Chicago, USA). The independent samples T test was applied to compare the two group, and one-way analysis of variance (ANOVA) was applied to compare the mean valuse among multiple group. Data were presented as the mean ± SD. $P < 0.05$ was considered statistically significant.

CRediT authorship contribution statement

Jing Zhao: Writing – original draft, Conceptualization, Validation, Investigation, Data curation. **Qiyue Jiang:** Data curation, Methodology. **Chunjie Xu:** Methodology. **Qiyue Jia:** Methodology. **Hongwei Wang:** Investigation. **Wenming Xue:** Investigation, Data curation. **Yan Wang:** Methodology. **Zhonghui Zhu:** Investigation. **Lin Tian:** Resources, Writing – review & editing, Project administration, Funding acquisition.

Declaration of Competing Interest

The authors declare that they have no known competing financial interests or personal relationships that could have appeared to influence the work reported in this paper.

Data availability

Data will be made available on request.

Acknowledgements

This study was supported by the National Natural Science Foundation of China under grants 82073522, 81872595.

Appendix A. Supporting information

Supplementary data associated with this article can be found in the online version at doi:10.1016/j.ecoenv.2023.114950.

References

Abbaszadeh, H., et al., 2020. Human umbilical cord mesenchymal stem cell-derived extracellular vesicles: A novel therapeutic paradigm. J. Cell. Physiol. 235, 706–717.
Ankrum, J.A., et al., 2014. Mesenchymal stem cells: immune evasive, not immune privileged. Nat. Biotechnol. 32, 252–260.
Calligaris, M., et al., 2021. Strategies to target ADAM17 in disease: from its discovery to the iRhom revolution. Mol. (Basel, Switz.) 26.
Cao, Z.-J., et al., 2022. Pirfenidone ameliorates silica-induced lung inflammation and fibrosis in mice by inhibiting the secretion of interleukin-17A. Acta Pharmacol. Sin. 43, 908–918.
Chanda, D., et al., 2019. Developmental pathways in the pathogenesis of lung fibrosis. Mol. Asp. Med. 65, 56–69.
Chen, S., et al., 2018. Transplantation of adipose-derived mesenchymal stem cells attenuates pulmonary fibrosis of silicosis via anti-inflammatory and anti-apoptosis effects in rats. Stem Cell Res. Ther. 9, 110.
Cheng, D., et al., 2021. Metformin attenuates silica-induced pulmonary fibrosis via AMPK signaling. J. Transl. Med. 19, 349.
Christian, L.M., 2012. The ADAM family: Insights into Notch proteolysis. Fly 6, 30–34.
Chung, Y.-H., et al., 2022. MiR-26a-5p as a useful therapeutic target for upper tract urothelial carcinoma by regulating WNT5A/β-catenin signaling. Sci. Rep. 12, 6955.
Cocozza, F., et al., 2020. SnapShot: extracellular vesicles. Cell 182, 262-262 e1.
Duffield, J.S., et al., 2013. Host responses in tissue repair and fibrosis. Annu. Rev. Pathol. 8, 241–276.
Fan, M., et al., 2022. A Novel N-Arylpyridone Compound Alleviates the Inflammatory and Fibrotic Reaction of Silicosis by Inhibiting the ASK1-p38 Pathway and Regulating Macrophage Polarization. Front Pharm. 13, 848435.
Ge, J., et al., 2020. Association of ADAM17 expression levels in patients with interstitial lung disease. Immunol. Invest 49, 134–145.
Huang, R., et al., 2020. The activation of GPER inhibits cells proliferation, invasion and EMT of triple-negative breast cancer via CD151/miR-199a-3p bio-axis. Am. J. Transl. Res. 12, 32–44.
Huang, Y., Yang, L., 2021. Mesenchymal stem cell-derived extracellular vesicles in therapy against fibrotic diseases. Stem Cell Res. Ther. 12, 435.
Kasai, H., et al., 2005. TGF-beta1 induces human alveolar epithelial to mesenchymal cell transition (EMT). Respir. Res. 6, 56.
Kim, K.K., et al., 2006. Alveolar epithelial cell mesenchymal transition develops in vivo during pulmonary fibrosis and is regulated by the extracellular matrix. Proc. Natl. Acad. Sci. USA 103, 13180–13185.
Li, D., et al., 2021. Human umbilical cord mesenchymal stem cell-derived exosomal miR-27b attenuates subretinal fibrosis via suppressing epithelial-mesenchymal transition by targeting HOXC6. Stem Cell Res. Ther. 12, 24.
Li, J., et al., 2019. Dual regulatory role of CCNA2 in modulating CDK6 and MET-mediated cell-cycle pathway and EMT progression is blocked by miR-381-3p in bladder cancer. FASEB J.: Off. Publ. Fed. Am. Soc. Exp. Biol. 33, 1374–1388.
Li, X., et al., 2017. Bone marrow mesenchymal stem cells attenuate silica-induced pulmonary fibrosis via paracrine mechanisms. Toxicol. Lett. 270.
Li, Y., et al., 2022. Mouse mesenchymal stem cell-derived exosomal miR-466f-3p reverses EMT process through inhibiting AKT/GSK3β pathway via c-MET in radiation-induced lung injury. J. Exp. Clin. Cancer Res.: CR 41, 128.
Liang, H., et al., 2014. Integrated analyses identify the involvement of microRNA-26a in epithelial-mesenchymal transition during idiopathic pulmonary fibrosis. Cell Death Dis. 5, e1238.
Liang, H., et al., 2016. miR-26a suppresses EMT by disrupting the Lin28B/let-7d axis: potential cross-talks among miRNAs in IPF. J. Mol. Med (Berl.) 94, 655–665.
Liu, J., et al., 2020. LncRNA KCNQ1OT1 knockdown inhibits viability, migration and epithelial-mesenchymal transition in human lens epithelial cells via miR-26a-5p/ITGAV/TGF-beta/Smad3 axis. Exp. Eye Res. 200, 108251.
Lu, H.Y., et al., 2019. Novel ADAM-17 inhibitor ZLDI-8 inhibits the proliferation and metastasis of chemo-resistant non-small-cell lung cancer by reversing Notch and epithelial mesenchymal transition in vitro and in vivo. Pharm. Res 148, 104406.
Ma, D.-N., et al., 2016. MicroRNA-26a suppresses epithelial-mesenchymal transition in human hepatocellular carcinoma by repressing enhancer of zeste homolog 2. J. Hematol. Oncol. 9, 1.
Nikitopoulou, I., et al., 2019. Orotracheal treprostinil administration attenuates bleomycin-induced lung injury, vascular remodeling, and fibrosis in mice. Pulm. Circ. 9, 2045894019881954.
Qi, Y., et al., 2020. miR-34a-5p Attenuates EMT through targeting SMAD4 in silica-induced pulmonary fibrosis. J. Cell. Mol. Med. 24, 12219–12224.
Qiu, Z., et al., 2022. Human umbilical cord mesenchymal stem cell-derived exosomal miR-335-5p attenuates the inflammation and tubular epithelial-myofibroblast transdifferentiation of renal tubular epithelial cells by reducing ADAM19 protein levels. Stem Cell Res. Ther. 13, 373.
Saad, S., et al., 2010. Notch mediated epithelial to mesenchymal transformation is associated with increased expression of the Snail transcription factor. Int J. Biochem Cell Biol. 42, 1115–1122.
Sensebé, L., Fleury-Cappellesso, S., 2013. Biodistribution of mesenchymal stem/stromal cells in a preclinical setting. Stem Cells Int. 2013, 678063.
Sheng, W., et al., 2020. Calreticulin promotes EMT in pancreatic cancer via mediating Ca dependent acute and chronic endoplasmic reticulum stress. J. Exp. Clin. Cancer Res.: CR 39, 209.
Shi, H., et al., 2021. MiR-26a-5p alleviates cardiac hypertrophy and dysfunction via targeting ADAM17. Cell Biol. Int. 45, 2357–2367.
Sisto, M., et al., 2021. ADAM 17 and Epithelial-to-Mesenchymal Transition: The Evolving Story and Its Link to Fibrosis and Cancer. J. Clin. Med. 10.
Sun, J., et al., 2019. MicroRNA-29b mediates lung mesenchymal-epithelial transition and prevents lung fibrosis in the silicosis model. molecular therapy. Nucleic Acids 14, 20–31.
The Lancet Respiratory, M., 2019. The world is failing on silicosis. Lancet Respir. Med. 7, 283.
Wang, X., et al., 2016. miR-148a-3p represses proliferation and EMT by establishing regulatory circuits between ERBB3/AKT2/c-myc and DNMT1 in bladder cancer. Cell Death Dis. 7, e2503.
Wang, Y., et al., 2021. Snail-mediated partial epithelial mesenchymal transition augments the differentiation of local lung myofibroblast. Chemosphere 267, 128870.
Wang, Z., et al., 2017. Specifically Formed Corona on Silica Nanoparticles Enhances Transforming Growth Factor β1 Activity in Triggering Lung Fibrosis. ACS Nano 11, 1659–1672.
Wiklander, O.P.B., et al., 2015. Extracellular vesicle in vivo biodistribution is determined by cell source, route of administration and targeting. J. Extracell. Vesicles 4, 26316.
Wiklander, O.P.B., et al., 2019. Advances in therapeutic applications of extracellular vesicles. Sci. Transl. Med. 11.
Xu, C., et al., 2020. Exosomes derived from three-dimensional cultured human umbilical cord mesenchymal stem cells ameliorate pulmonary fibrosis in a mouse silicosis model. Stem Cell Res Ther. 11, 503.
Xu, C., et al., 2022. Exosomal let-7i-5p from three-dimensional cultured human umbilical cord mesenchymal stem cells inhibits fibroblast activation in silicosis through targeting TGFBR1. Ecotoxicol. Environ. Saf. 233, 113302.
Yaghoubi, Y., et al., 2019. Human umbilical cord mesenchymal stem cells derived-exosomes in diseases treatment. Life Sci. 233, 116733.
Yang, S., et al., 2022. Every road leads to Rome: therapeutic effect and mechanism of the extracellular vesicles of human embryonic stem cell-derived immune and matrix regulatory cells administered to mouse models of pulmonary fibrosis through different routes. Stem Cell Res Ther. 13, 163.
Zhang, J., et al., 2012. MicroRNA-26a promotes cholangiocarcinoma growth by activating β-catenin. Gastroenterology 143.
Zhang, Z., et al., 2020. The protective effects of MSC-EXO against pulmonary hypertension through regulating Wnt5a/BMP signalling pathway. J. Cell. Mol. Med. 24, 13938–13948.